Optimal noninvasive measurement of full counting statistics by a single qubit

A. V. Lebedev,[1] G. B. Lesovik,[2] and G. Blatter[1]

[1]*Theoretische Physik, Wolfgang-Pauli-Strasse 27, ETH Zurich, CH-8093 Zürich, Switzerland*

[2]*L. D. Landau Institute for Theoretical Physics Russian Academy of Sciences, Akad. Semenova Avenue, 1-A, Chernogolovka 142432, Moscow Region, Russia*

(Received 11 December 2015; published 24 March 2016)

The complete characterization of the charge transport in a mesoscopic device is provided by the full counting statistics (FCS) $P_t(m)$, describing the amount of charge $Q = me$ transmitted during the time t. Although numerous systems have been theoretically characterized by their FCS, the experimental measurement of the distribution function $P_t(m)$ or its moments $\langle Q^n \rangle$ is rare and often plagued by strong back-action. Here, we present a strategy for the measurement of the FCS, more specifically its characteristic function $\chi(\lambda)$ and moments $\langle Q^n \rangle$, by a qubit with a set of different couplings λ_j, $j = 1, \ldots, k, \ldots k + p, k = \lceil n/2 \rceil$, $p \geqslant 0$, to the mesoscopic conductor. The scheme involves multiple readings of Ramsey sequences at the different coupling strengths λ_j, and we find the optimal distribution for these couplings λ_j as well as the optimal distribution N_j of $N = \sum N_j$ measurements among the different couplings λ_j. We determine the precision scaling for the moments $\langle Q^n \rangle$ with the number N of invested resources and show that the standard quantum limit can be approached when many additional couplings $p \gg 1$ are included in the measurement scheme.

DOI: 10.1103/PhysRevB.93.115140

I. INTRODUCTION

Traditionally, electronic transport through a device is characterized by the current and its noise. Within mesoscopic physics, Landauer's scattering matrix approach [1] provides a very physical and straightforward technique for the calculation of the average current [1–4] and noise [5–9], as well as higher moments. The quantity which fully characterizes the random process of charge transport is given by the so-called full counting statistics (FCS), telling what charge $Q = me$ is transmitted through the device during a fixed time t [10]. The first calculation [11] of the probability distribution function $P_t(m)$ for the FCS goes back to 1992 and was quickly developed further [12–14]. Various generalizations and applications have been proposed, e.g., the current noise in a normal-metal–superconductor point contact [15], the electron transfer between superconductors [16], charge pumping [17] and charge transfer [18] in the Coulomb blockade regime, the extension to energy-dependent scatterers [19], the statistical properties of the persistent current in nanostructures [20], and the fluctuations in the heat current in a quantum conductor [21] or between two superconductors [22], to name just a few of the numerous theoretical studies. At the same time, there are only very few experiments measuring higher-order correlators [23–25] and one set of experiments measuring directly the statistics [26–29]. Unfortunately, measurement back-action is substantial in all of these experiments and a noninvasive measurement of the full counting statistics remains to be done. An early suggestion, formulated on the level of a Gedanken experiment and involving a spin [14], has later given way to a more concrete proposal based on charge or flux qubits [30]. However, a specific protocol how such a qubit is used in an optimal fashion is missing and it is the purpose of the present paper to close this gap.

The distribution function $P_t(m)$ and its moments or cumulants can be obtained from the generating function $\chi_t(\lambda)$, the Fourier transform of $P_t(m)$, $\chi_t(\lambda) = \sum_m P_t(m) \exp(im\lambda)$. Here, λ not only represents a compact variable in the Fourier transform, but in its physical role it appears as the coupling constant between the transported charge and the qubit detector (here, we have in mind any qubit that couples to the charge either inductively or capacitively). The basic quantity we are interested in then is the generating function $\chi(\lambda)$ and its derivatives with respect to λ. The latter define the moments (or cumulants) of the distribution function $P(m)$ [here and below we drop the time-index t on $P_t(m)$ and $\chi_t(\lambda)$]. The issue is to find the generating functions from measured data. This involves a simple protocol on the qubit with preparation, measurement, and a binary readout—the probabilities $P_\pm$ for the binary outcomes $+$ or $-$ at fixed λ then allow for a statistical estimate $\tilde{\chi}(\lambda)$ of the generating function $\chi(\lambda)$. Evaluating $\tilde{\chi}(\lambda)$ for various values $\lambda = \lambda_j$ then allows for the determination of derivatives $\partial_\lambda^n \tilde{\chi}(\lambda)$ via finite-difference formulas, from which estimates for the moments $\langle Q^n \rangle$ or cumulants can be obtained. The main question we want to answer in this paper then is, given a total of N measurements, what is the optimal way to carry out these measurements? In particular, what number and distribution of grid points λ_j shall be chosen, how should the N measurements be distributed among the grid points, what accuracy can be achieved, and how does the precision of the result scale with the number N of invested resources or measurements?

In Sec. II below, we will first describe the measurement protocol providing estimates for the real and imaginary parts of the characteristic function $\chi(\lambda)$ and analyze the statistical distribution (or precision) of the measured results. The moments of transferred charge involve higher-order derivatives of the characteristic function $\chi(\lambda)$ and Sec. III is devoted to their construction out of measured values of χ through finite-difference formulas. The choice of grid points in these finite-difference formulas interferes with the statistical errors from the measurements and one has to find the optimal grid and measurement strategy to minimize the total error for the charge moments; this task is discussed in Sec. III A for an equidistant set of coupling strengths and in Sec. III B for a

nonequidistant set of grid points. The optimal measurement strategy involves a nonequidistant set of points and we find the optimal distribution of the number of measurements as well as the precision scaling with the total number N of measurements. Specific results in the form of tables are given for the measurement of the third-order cumulant $\langle Q^3\rangle$. In Sec. IV we present a summary, emphasize our main results, and add some concluding remarks on the use of different types of qubits and the relation to quantum counting [31,32].

II. MEASUREMENT OF THE CHARACTERISTIC FUNCTION

The full counting statistics of a conductor can be described through the set of probabilities $P_t(m)$ to transmit m particles (electrons) in a given time t (in the following we drop the index t). The discrete probability distribution $P(m)$ can be characterized by a continuous generating function $\chi(\lambda) = \sum_m P(m)e^{im\lambda}$. Given the generating function $\chi(\lambda)$, one can find all moments of the transmitted charge (with the charge Q measured in units of e),

$$\mathcal{Q}_n \equiv \langle \hat{Q}^n\rangle = (-i)^n \lim_{\lambda\to 0} \partial_\lambda^n \chi(\lambda), \tag{1}$$

or the charge cumulants,

$$\mathcal{K}_n \equiv \langle\langle \hat{Q}^n\rangle\rangle = (-i)^n \lim_{\lambda\to 0} \partial_\lambda^n \ln\chi(\lambda). \tag{2}$$

In order to find the above quantities in an experiment, we consider a qubit locally interacting with the conductor as described by the Hamiltonian $\hat{H}_{\rm int} = (\hbar\lambda/e)\hat{\sigma}_z\hat{I}(x,t)$, where $\hat{I}(x,t)$ is the electric current operator in the conductor providing the transmitted charge at a position x behind the scatterer (see Fig. 1 for an illustration). Such a linear coupling is appropriate when the interaction point x resides away from the scattering region in the conductor (see Bachmann *et al.* [33]). The qubit-current interaction leads to a rotation of the qubit state around the z axis by an angle $\varphi = m\lambda$, where m is the transmitted charge. Consider a standard Ramsey sequence of qubit rotations $\hat{R}(\varphi) = \hat{U}_y(-\pi/2)\hat{U}_z(\varphi)\hat{U}_y(\pi/2)$, where $\hat{U}_{\vec{n}}(\alpha) = \hat{\mathbb{1}}\cos(\alpha/2) - i\vec{n}\cdot\hat{\vec{\sigma}}\sin(\alpha/2)$, where the first and last rotations describe $\pm\pi/2$ rotations around the y axis and the intermediate rotation is due to the interaction with the conductor. Applying this Ramsey sequence to an initial qubit state $|\uparrow\rangle$ (with $\sigma_z = 1$), one arrives at the final state:

$$|m\rangle = \hat{R}(\varphi = m\lambda)|\uparrow\rangle = \cos\frac{m\lambda}{2}|\uparrow\rangle + i\sin\frac{m\lambda}{2}|\downarrow\rangle. \tag{3}$$

The probabilities to observe the qubit in a state $\sigma_z = \pm 1$ then are given by

$$P_\pm(m\lambda) = \tfrac{1}{2} \pm \tfrac{1}{2}e^{-t/\tau_\varphi}\cos(m\lambda). \tag{4}$$

The exponential damping in Eq. (4) accounts for the finite dephasing time τ_φ of the qubit that we may model through a stochastic Gaussian H field. Such a finite dephasing time τ_φ ultimately limits the time t during which the FCS $P_t(m)$ can be measured. For a particular run of the Ramsey sequence, the random number m of transmitted charges is unknown but governed by the FCS distribution $P(m)$, hence the probabilities for the two final qubit states can be found by averaging over m:

$$P_\pm(\lambda) = \sum_m P(m)\, P_\pm(m\lambda). \tag{5}$$

These probabilities are conveniently expressed through the real part of the FCS characteristic function:

$$P_\pm(\lambda) = \tfrac{1}{2} \pm \tfrac{1}{2}e^{-t/\tau_\varphi}{\rm Re}\chi(\lambda). \tag{6}$$

Hence, repeating the Ramsey sequence $N \gg 1$ times and observing $N_\pm$ final outcomes with $\sigma_z = \pm 1$, one can directly estimate the real part of the characteristic function for a given dimensionless interaction parameter λ:

$$e^{-t/\tau_\varphi}{\rm Re}\tilde{\chi}(\lambda) = \frac{N_+ - N_-}{N_+ + N_-}, \tag{7}$$

where the tilde $\tilde{\chi}(\lambda)$ refers to a statistical estimate of $\chi(\lambda)$. The imaginary part of the characteristic function can be estimated in a similar way by applying the alternative Ramsey sequence $\hat{R}'(\varphi) = \hat{U}_x(-\pi/2)\hat{U}_z(\varphi)\hat{U}_x(\pi/2)$ to the initial state $\sigma_z = 1$ of the qubit.

In a realistic situation, the $\pi/2$ pulses in the Ramsey sequence are not perfect, which modifies the statistical analysis of the data. Let us consider a nonperfect Ramsey sequence $\hat{R}(\varphi) = \hat{U}_y(-\pi/2+\delta')\hat{U}_z(\varphi)\hat{U}_y(\pi/2-\delta)$ with small deviations δ and δ'. As a result, the perfect qubit probabilities $P_\pm(\lambda)$ in Eq. (6) are modified:

$$P_\pm(\lambda) = \frac{1 \pm \sin\delta\sin\delta'}{2} \pm \frac{e^{-t/\tau_\varphi}\cos\delta\cos\delta'}{2}{\rm Re}\chi(\lambda). \tag{8}$$

The imperfect $\pi/2$ pulses affect the result in two ways: (i) an effective decrease of the visibility factor, $e^{-t/\tau_\varphi} \to e^{-t/\tau_\varphi}\cos(\delta)\cos(\delta')$, which amounts to a renormalized dephasing time $\bar{\tau}_\varphi$ (at fixed t), and (ii) a finite bias $P_+ - P_- = \sin(\delta)\sin(\delta')$ at $\lambda = 0$ that can be accounted for with a separate measurement. As a result, the estimated value of the characteristic function is given by

$$e^{-t/\bar{\tau}_\varphi}{\rm Re}\tilde{\chi}(\lambda) = \left.\frac{N_+ - N_-}{N_+ + N_-}\right|_\lambda - \left.\frac{N_+ - N_-}{N_+ + N_-}\right|_0. \tag{9}$$

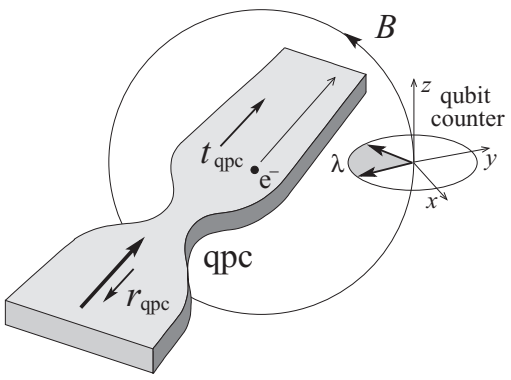

FIG. 1. Measurement of transmitted charge, e.g., across a quantum point contact with transmission and reflection amplitudes $t_{\rm qpc}$ and $r_{\rm qpc}$, respectively, by a qubit. The passage of an electron through the outgoing conductor generates a magnetic field pulse that rotates the qubit state (drawn as a vector on the Bloch sphere) by λ.

Note that the uncertainty in the dephasing time shows up in the final results with a small power $\alpha_{n,p}$ [see, e.g., Eq. (29)]. In the following, we will assume perfect pulses with $\delta = 0 = \delta'$.

Next, we derive the statistical bounds for the estimation of $\tilde{\chi}$. The experimental outcomes $N_\pm$ are distributed according to a binomial distribution, $P(N_+,N_-) = C_N^{N_+}[P_+(\lambda)]^{N_+}[P_-(\lambda)]^{N_-}$. As follows from Eq. (6) this distribution can be characterized by a single parameter $x = \exp(-t/\tau_\varphi)\mathrm{Re}\chi(\lambda)$ or $x = \exp(-t/\tau_\varphi)\mathrm{Im}\chi(\lambda)$. Hence, by virtue of the Bayes theorem and observing a particular set $N_\pm$ of results $\sigma_z = \pm 1$, one can obtain an estimate of the *posterior* distribution function for the unknown parameter $x \in [-1,1]$ via

$$P(x|N_+,N_-) = \frac{(N+1)!}{2N_+!N_-!}\left(\frac{1+x}{2}\right)^{N_+}\left(\frac{1-x}{2}\right)^{N_-}. \quad (10)$$

For large $N_\pm$, the above distribution approaches a Gaussian, $P(x|N_+,N_-) \to \mathcal{N}(\tilde{x},\sigma^2)$ with mean $\tilde{x} = [N_+ - N_-]/N$ and variance $\sigma^2 = 4N_+N_-/N^3 = (1-\tilde{x}^2)/N$. Then, the statistical bounds for the estimated mean $x \approx \tilde{x}$ at a given tolerance level ϵ are given by

$$\mathrm{Prob}[|x-\tilde{x}| \leqslant g(\epsilon)\sigma] = 1-\epsilon, \quad (11)$$

where $g(\epsilon)$ is determined by $1-\epsilon = \mathrm{erf}(g/\sqrt{2})$ and the standard error function $\mathrm{erf}(x) = (1/\sqrt{\pi})\int_{-x}^{x} dt\, e^{-t^2}$, quickly approaching unity at large x, $\mathrm{erf}(2) \approx 0.995$. Going back from the variable x to the characteristic function $\chi(\lambda)$, one finds that with a probability $1-\epsilon$

$$|\mathrm{Re}\chi(\lambda) - \mathrm{Re}\tilde{\chi}(\lambda)| \leqslant g(\epsilon)\frac{v_{\mathrm{Re}}(\lambda)}{\sqrt{N}}, \quad (12)$$

where $v_{\mathrm{Re}}^2(\lambda) = \exp(2t/\tau_\varphi) - [\mathrm{Re}\tilde{\chi}(\lambda)]^2$ increases exponentially when pushing the measurement time beyond τ_φ. The same estimate holds true for the imaginary part of $\chi(\lambda)$. The above measurement procedure then reaches the precision of the standard quantum limit at large N. We will see below that carrying over this standard quantum limit in the measurement precision for the moments $\mathcal{Q}_n$ is a nontrivial task [due to the appearance of derivatives $\partial_\lambda^n\chi(\lambda)$] and requires special measures.

Special attention has to be paid to the situation at small coupling $\lambda \gtrsim 0$, where $\mathrm{Re}\chi(0) = 1$ and $\mathrm{Im}\chi(0) = 0$. The latter poses no problem as the distribution function Eq. (10) is centered around $x = 0$, away from the boundaries at $x = \pm 1$, and hence well approximated by a Gaussian distribution with $v_{\mathrm{Im}}^2(\lambda) \leqslant v_{\mathrm{Im}}^2(0) \approx e^{2t/\tau_\varphi}$. In contrast, when measuring the real part $\mathrm{Re}\chi(\lambda \gtrsim 0)$, the distribution function (10) is squeezed towards the boundary at $x = 1$. In this situation, $N_+ \sim N$ and Eq. (10) can be approximated by

$$P(x|N_+,N_-) = \frac{N_+^{N_-+1}}{2N_-!}\left(\frac{1-x}{2}\right)^{N_-}e^{-N_+(1-x)/2}. \quad (13)$$

The maximum of Eq. (13) is attained at $\tilde{x} = 1 - 2N_-/N_+$ and provides an estimate for x with an accuracy quantified by the variance $\sigma^2 = 4(N_- + 1)/N_+^2$ and a precision scaling as $1/N$. With increasing N, the number N_- of outcomes $\sigma_z = -1$ increases and the distribution (10) detaches from $x = 1$ with Eq. (13) providing no longer a good approximation. Rather, the distribution (10) approaches the standard Gaussian form when $1-\tilde{x}$ becomes larger than σ, which is the case for $N_- \gg 1$ (using either of the above estimates for $\tilde{x}$ and σ). In the following, we assume that N is large enough, such that the Gaussian approximation for the random variable $x = e^{-\tau/\tau_\varphi}\mathrm{Re}\chi(\lambda)$ provides a good description at any coupling strength $\lambda > 0$.

III. CALCULATION OF DERIVATIVES

Following Eq. (1), the characteristic function $\chi(\lambda)$ (and its estimate $\tilde{\chi}$) can be used to determine the charge moments $\mathcal{Q}_n$. This requires taking nth-order derivatives of $\chi(\lambda)$ near $\lambda = 0$, which can be found with the help of finite-difference formulas of the form

$$\partial_\lambda^n\chi(\lambda)|_{\lambda=0} \equiv \chi^{(n)}(0) \approx \sum_{\lambda\in\Lambda} w_\lambda^{(n)}\,\chi(\lambda), \quad (14)$$

where $w_\lambda^{(n)}$ is a set of weight coefficients and $\Lambda = \{\lambda_0,\lambda_1,\ldots\lambda_m\}$ with $m \geqslant n$ is a set of λ values near the origin $\lambda = 0$. For a given Λ and n, one can find the corresponding weight coefficients w_λ (here and below we drop the index $^{(n)}$ on $w_\lambda^{(n)}$) using the procedure described in Ref. [34]: defining $\omega(x) \equiv \prod_{\lambda\in\Lambda}(x-\lambda)$, these are given as

$$w_\lambda = \frac{d^n}{dx^n}\frac{\omega(x)}{\omega'(\lambda)(x-\lambda)}\bigg|_{x=0} \quad (15)$$

with $\omega'(x) = \partial_x\omega(x)$. The characteristic function $\chi(\lambda)$ is the Fourier transform of a real distribution function P_n and hence $\chi(\lambda) = \chi^*(-\lambda)$. This symmetry motivates the use of symmetric sets $\Lambda_{n,p} = \{-\lambda_{k+p},\ldots,-\lambda_1,0,\lambda_1,\ldots,\lambda_{k+p}\}$, where $n = 2k$ or $n = 2k-1$ refer to even- or odd-order derivatives with $k > 0$ and $p \geqslant 0$. This particular choice of the grid set $\Lambda_{n,p}$ twice reduces the number of points where $\chi(\lambda)$ has to be measured. Indeed, using Eq. (15), one shows that $w_\lambda = w_{-\lambda}$ for even n and $w_\lambda = -w_{-\lambda}$ when n is odd. In addition, $\chi(0) = 1$ and one needs to measure $\chi(\lambda)$ only at the $k+p$ points λ_j with $j = 1,\ldots,k+p$. Using the symmetry of the characteristic function $\chi(\lambda)$, the even (odd) derivatives of the characteristic function can be expressed through its real (imaginary) parts, respectively:

$$\chi^{(n)}(0) \approx \begin{cases} w_0 + 2\sum_{j=1}^{k+p} w_{\lambda_j}\mathrm{Re}\chi(\lambda_j), & n = 2k \\ 2i\sum_{j=1}^{k+p} w_{\lambda_j}\,\mathrm{Im}\chi(\lambda_j), & n = 2k-1 \end{cases}. \quad (16)$$

Making use of the Gaussian distributed estimates $\mathrm{Re}\chi(\lambda_j)$ and $\mathrm{Im}\chi(\lambda_j)$ characterized by Eq. (12) the numerical derivatives Eq. (16) are Gaussian random variables as well with a variance,

$$\mathrm{Var}[\chi^{(n)}(0)] = 4g^2(\epsilon)\sum_{j=1}^{k+p}\frac{[w_{\lambda_j}v_n(\lambda_j)]^2}{N_j}, \quad (17)$$

where $v_n(\lambda)$ is equal to $v_{2k} = v_{\mathrm{Re}}$ ($v_{2k-1} = v_{\mathrm{Im}}$) for even (odd) derivatives n and N_j is the number of measurements that has been used to estimate the value of the characteristic function at $\lambda = \lambda_j$. Given a total number of measurements $N = \sum_j N_j$, the question poses itself how to distribute these resources over the $k+p$ measurement points. Minimizing $\mathrm{Var}[\chi^{(n)}(0)]$ under the condition of fixed N one derives the following expression for the ratios $r_j \equiv N_j/N$ optimizing the

distribution of measurements,

$$r_j = \frac{|w_{\lambda_j}|v_n(\lambda_j)}{\sum_{l=1}^{k+p}|w_{\lambda_l}|v_n(\lambda_l)}, \tag{18}$$

and the minimal variance is given by

$$\delta\mathcal{Q}_n^2 \equiv \mathrm{Var}[\chi^{(n)}(0)] = \frac{4g^2(\epsilon)}{N}\left[\sum_{j=1}^{k+p}|w_{\lambda_j}|v_n(\lambda_j)\right]^2. \tag{19}$$

Having established the statistical error in the estimates of the derivatives of χ, one also needs to take into account a second type of error arising due to approximation given by the finite-difference formulas. E.g., choosing the grid points $\lambda \in \Lambda$ close to the origin $\lambda = 0$ decreases the error in the finite-difference approximation [since the remainder in the approximation (14) is of order λ^{n+p+2}]; however, the statistical error Eq. (19) grows due to the larger weights $w_\lambda \propto 1/\lambda^n$. Hence, we have to find the optimal grid Λ_{opt} that minimizes the total error given by the sum of statistical and approximation errors. This minimization introduces a dependence $\lambda_j(N)$ which will change (i.e., reduce) the overall precision scaling for the moments away from the standard quantum limit.

A. Equidistant grids

Consider a measurement of the nth moment of transferred charge $\mathcal{Q}_n$ by a set of $k+p$ qubits with equidistant coupling strengths $\lambda_j = j\lambda_0$, $j = 1,\ldots,k+p$, where $n = 2k$ or $2k-1$ and $p \geqslant 0$. Making use of Eq. (15), the weights w_{λ_j} in the finite-difference formulas (16) can be written in the form $w_{\lambda_j} = \kappa_j/\lambda_0^n$, where the coefficients κ_j denote the set of numbers

$$\kappa_j = \frac{d^n}{dx^n}\frac{\omega(x)}{\omega'(j)(x-j)}\bigg|_{x=0} \tag{20}$$

with $\omega(x) = x\prod_{j=1}^{k+p}(x^2-j^2)$. Making use of Eq. (17), the statistical error of the measurement then is given by

$$\delta\mathcal{Q}_n^2\big|_{\mathrm{stat}} = \frac{4g^2(\epsilon)}{\lambda_0^{2n}N}\sum_{j=1}^{k+p}\frac{\kappa_j^2}{r_j}v_n^2(j\lambda_0).$$

In the following, we approximate $v_{2k-1}(\lambda) \approx e^{\tau/\tau_\varphi}$ and $v_{2k}(\lambda) \approx e^{\tau/\tau_\varphi} - 1$, hence we assume that $v_n(\lambda)$ no longer depends on λ near the origin; since $v_n(0) \leqslant v_n(\lambda)$, this corresponds to a conservative estimate of the statistical error.

The approximation error $\delta\mathcal{Q}_n|_{\mathrm{approx}}$ originating from the finite-difference formula approximating the derivative can be obtained from Eq. (16) by substituting the Taylor expansion of $\mathrm{Re}\chi(j\lambda_0)$ or $\mathrm{Im}\chi(j\lambda_0)$; the first $n+2p$ terms in this weighted (with the coefficients w_{λ_j}) sum vanish (due to the very definition of the weights w_{λ_j}) and the next term $\propto \lambda_j^{n+2p+2}$ provides an estimate for the remainder

$$\delta\mathcal{Q}_n\big|_{\mathrm{approx}} = \lambda_0^{2p+2}\,|\mathcal{Q}_{n+2p+2}|\,\beta_{n,p}, \tag{21}$$

with the numerical (here, we introduce the coefficients $\nu_j = j$ for later reference; see Sec. III B)

$$\beta_{n,p} = 2\frac{\left|\sum_{j=1}^{k+p}\nu_j^{n+2p+2}\kappa_j\right|}{(n+2p+2)!}. \tag{22}$$

Minimizing the total error $\delta\mathcal{Q}_n = \delta\mathcal{Q}_n|_{\mathrm{stat}} + \delta\mathcal{Q}_n|_{\mathrm{approx}}$ with respect to λ_0, we find the minimal error

$$\delta\mathcal{Q}_n(\bar\lambda_0) = A_{n,p}\,|\mathcal{Q}_{n+2p+2}|^{1-2\alpha_{n,p}}\left[\frac{g^2(\epsilon)v_n^2}{N}\right]^{\alpha_{n,p}}, \tag{23}$$

with the scaling exponent

$$\alpha_{n,p} = \frac{p+1}{n+2p+2} \tag{24}$$

and the optimal distance $\bar\lambda_0$ between the couplings λ_j:

$$\bar\lambda_0 = B_{n,p}\left[\frac{g(\epsilon)v_n}{|\mathcal{Q}_{n+2p+2}|\sqrt{N}}\right]^{\alpha_{n,p}/(p+1)}. \tag{25}$$

The exponent $1/(n+2) \leqslant \alpha_{n,p} < 1/2$ describes the precision scaling of the experiment with the number N of measurements. The numericals $A_{n,p}$ and $B_{n,p}$ are given by the expressions

$$A_{n,p} = \frac{p+1}{n}\frac{\beta_{n,p}}{\alpha_{n,p}}[S_{n,p}]^{\alpha_{n,p}}, \tag{26}$$

$$B_{n,p} = [S_{n,p}]^{\alpha_{n,p}/2(p+1)}, \tag{27}$$

with

$$S_{n,p} = \frac{n^2\sum_{j=1}^{k+p}\kappa_j^2/r_j}{(p+1)^2\beta_{n,p}^2}. \tag{28}$$

Finding the nth-order moment of the transmitted charge requires measuring $\mathrm{Re}\chi(\lambda)$ or $\mathrm{Im}\chi(\lambda)$ in at least at k different values of the coupling constant λ. Analyzing the scaling of the net error (23) with respect to the number N of measurements, one notes that using only a minimal number of points, i.e., $p = 0$, produces a small scaling exponent $\alpha_{n,0} = 1/(n+2)$, and hence reaching a good precision implies a large number N of measurements. In order to achieve a shorter overall duration of the experiment one needs to add more measurement points $p > 0$; this strategy then allows one to reach the standard quantum limit $\delta\mathcal{Q}_n \propto 1/\sqrt{N}$ at large p.

Next, let us estimate the optimal coupling parameter $\bar\lambda_0$ as given by Eq. (25). Assuming a driven (or nonequilibrium) charge transport, the higher moments scale as $|\mathcal{Q}_{n+2p+2}| \sim |\bar Q|^{n+2p+2}$ with $\bar Q = \mathcal{Q}_1$ denoting the average transmitted charge (in units of e). Then,

$$\bar\lambda_0 \sim \frac{B_{n,p}}{|\bar Q|}\left[\frac{g(\epsilon)v_n}{\sqrt{N}}\right]^{\alpha_{n,p}/(p+1)}, \tag{29}$$

and the relative accuracy of the nth moment $\delta\mathcal{Q}_n/|\mathcal{Q}_n| \sim \delta\mathcal{Q}_n/|\bar Q|^n$ is given by

$$\frac{\delta\mathcal{Q}_n}{|\bar Q|^n} = A_{n,p}\left[\frac{g^2(\epsilon)v_n^2}{N}\right]^{\alpha_{n,p}}. \tag{30}$$

Optimizing the proposed measurement scheme then requires a weak coupling λ between the conductor and the qubit, implying that the qubit is typically rotated by an angle $\varphi \sim \bar Q\bar\lambda_0 \sim 1$ in the xy plane of the Bloch sphere during one Ramsey sequence (given the smallness of the exponent, we drop the factor $N^{-\alpha_{n,p}/2(p+1)}$). This result is quite natural, since at large couplings λ the qubit would perform multiple 2π rotations which cannot be distinguished by the proposed measurement scheme.

TABLE I. Weight factors κ_j, scaling exponent $\alpha_{3,p}$, and numericals $A_{3,p}$ and $B_{3,p}$ determining the third moment of transmitted charge for different additional grid points p.

p	κ_1	κ_2	κ_3	κ_4	κ_5	$\alpha_{3,p}$	$A_{3,p}$	$B_{3,p}$
0	-1	$\frac{1}{2}$	0	0	0	$\frac{1}{5}$	1.32	1.78
1	$-\frac{13}{8}$	1	$-\frac{1}{8}$	0	0	$\frac{2}{7}$	1.55	1.84
2	$-\frac{61}{30}$	$\frac{169}{120}$	$-\frac{3}{10}$	$\frac{7}{240}$	0	$\frac{1}{3}$	1.73	1.87
3	$-\frac{1669}{720}$	$\frac{4369}{2520}$	$-\frac{541}{1120}$	$\frac{1261}{15120}$	$-\frac{41}{6048}$	$\frac{4}{11}$	1.89	1.89

1. Third-order charge moment

Let us consider in more detail the measurement of the third-order charge moment $\mathcal{Q}_3$ ($n=3, k=2$) for an equidistant grid with a different number of points $2+p$, $p=0,1,\ldots$. The corresponding weight factors in Eq. (20), scaling exponent $\alpha_{3,p}$, and scaling factors $A_{3,p}$ and $B_{3,p}$ are presented in Table I for $p=0,1,2,3$. Note that the numericals $A_{3,p}$ and $B_{3,p}$ are all of order unity.

The weights κ_j in the finite-difference approximation assume higher absolute values near the origin (small j) and are almost vanishing at large j. Therefore, most measurements have to be done for the first few grid points near the origin $\lambda=0$; the relative number $r_j=N_j/N$ of measurements [as they follow from Eq. (18)], are summarized in Table II [the point $\lambda_0=0$ requires no measurement as $\chi(0)=1$].

B. Nonequidistant grids

An equidistant set of grid points may not provide the optimal result, i.e., the smallest error $\delta\mathcal{Q}_n$. Hence, let us parametrize a nonequidistant set of couplings $\Lambda=\lambda_0\{1,\nu_2,\nu_3,\ldots,\nu_{k+p}\}$ by the minimal coupling λ_0 and an ordered set of $k+p$ constants $\nu_1=1<\nu_2<\cdots<\nu_{k+p}$. According to Eq. (15), the finite-difference weights w_{λ_j} have the form $w_{\lambda_j}=\kappa_j/\lambda_0^n$ where κ_j can be found from Eq. (20) with

$$\omega(x)=x\prod_{j=1}^{k+p}\left(x^2-\nu_j^2\right). \tag{31}$$

Repeating the above analysis, one can minimize the sum of statistical and approximation errors as a function of the coupling strength parameter λ_0. The results (23) and (25) then hold true for the general grid Λ with the replacement of the coefficients $\nu_j=j$ in Eq. (22) by the distance coefficients ν_j. Dropping the requirement of equidistant grid points, one may attempt to further optimize the factor $A_{n,p}$ in Eq. (23)

TABLE II. Relative number of measurements $r_j=N_j/N$ for the jth grid point.

p	r_1	r_2	r_3	r_4	r_5
0	$\frac{2}{3}$	$\frac{1}{3}$	0	0	0
1	0.59	0.36	0.05	0	0
2	0.539	0.373	0.080	0.008	0
3	0.5012	0.3749	0.1044	0.0180	0.0015

for given n and p. Although we have not been able to find an analytic expression for the coefficients ν_j, we have performed a numerical optimization of $A_{n,p}$ for $n=3$ and $p=0,1,2,3$ as a function of ν_j with the results shown in Table III (the relative number r_j of measurements remain those given in Table II).

C. Coupling strength sensitivity

Another experimental limitation is due to imperfect knowledge of the coupling strengths λ_j. Assuming an accuracy $\delta\lambda_j$, the weight coefficients w_{λ_j} inherit an imprecision

$$\delta w_{\lambda_j}=\sum_{l=1}^{k+p}\frac{\partial w_{\lambda_j}}{\partial\lambda_l}\,\delta\lambda_l \tag{32}$$

and the resulting variation of the charge moment is given by

$$\delta\mathcal{Q}_n^2=\sum_{l=1}^{k+p}\frac{\delta\lambda_l^2}{\lambda_l^2}\left[\sum_{j=1}^{k+p}\lambda_l\frac{\partial w_{\lambda_j}}{\partial\lambda_l}\,\mathrm{Im}\chi(\lambda_j)\right]^2 \tag{33}$$

for the odd charge moments and a similar expression holds for the even moments. A conservative estimate is obtained by replacing $|\chi(\lambda)|^2\leqslant 1$ by unity in the above formula. The derivatives $\lambda_l\partial_{\lambda_l}w_{\lambda_j}=(\nu_l/\lambda_0^n)\partial_{\nu_l}\kappa_j$ can be found (numerically) from Eq. (20) for a given set Λ of coupling strengths. For simplicity, we assume that all coupling parameters λ_j are known with the same relative accuracy $\epsilon_\lambda=\delta\lambda_j/\lambda_j$; then

$$\delta\mathcal{Q}_n^2\leqslant\frac{E_{n,p}^2}{\bar\lambda_0^{2n}}\,\epsilon_\lambda^2, \tag{34}$$

where we have replaced λ_0 by $\bar\lambda_0$ [see Eq. (29)], and

$$E_{n,p}^2=\sum_{l=1}^{k+p}\left[\sum_{j=1}^{k+p}\nu_l\frac{\partial\kappa_j}{\partial\nu_l}\right]^2 \tag{35}$$

is a numerical factor which depends only on the set of relative coupling strengths ν_j. Given a relative accuracy ϵ_λ, one can find the total number of measurements $\bar N$ required to give the same measurement precision $\delta\mathcal{Q}_n$ as in Eq. (30):

$$\bar N\sim\left[g(\epsilon)\,v_{\mathrm{Im}}\frac{A_{n,p}B_{n,p}^n}{E_{n,p}}\right]^2\frac{1}{\epsilon_\lambda^2}. \tag{36}$$

A further increase of N beyond $\bar N$ does not improve the precision of $\mathcal{Q}_n$. In Table IV below, we list the corresponding factors $E_{3,p}$ for the measurement of the third-order charge moment with an equidistant and an optimal grid. Note that the measurement involving the optimal grid is less sensitive to the errors in λ_j as compared with the measurement based on the equidistant grid and requires less measurements $\bar N$. For example, the measurement with $p=3$ provides a scaling exponent $\alpha_{3,3}=4/11$ and using a nonequidistant optimal grid one arrives at the results

$$\bar N\approx 17.2\frac{g^2(\epsilon)v_{\mathrm{Im}}^2}{\epsilon_\lambda^2},\quad \frac{\delta\mathcal{Q}_3}{|\bar Q|^3}\sim 0.21\,\epsilon_\lambda^{8/11}, \tag{37}$$

TABLE III. Optimal grid coefficients v_j, weight factors κ_j, and numericals $A_{3,p}$ and $B_{3,p}$ determining the third moment of transmitted charge for an additional number of grid points $p = 0,1,2,3$.

p	v_2	v_3	v_4	v_5	κ_1	κ_2	κ_3	κ_4	κ_5	$A_{3,p}$	$B_{3,p}$
0	2.6180				−0.5125	0.1957				1.29	1.40
1	2.8019	4.0488			−0.6897	0.3182	−0.0499			1.46	1.36
2	2.8793	4.4113	5.4113		−0.7676	0.3770	−0.0941	0.0180		1.59	1.33
3	2.9188	4.6013	5.9109	6.7417	−0.8082	0.4087	−0.1208	0.0380	−0.0080	1.68	1.31

while using an equidistant grid leads to values

$$\bar{N} \approx 18.8 \frac{g^2(\epsilon) v_{\mathrm{Im}}^2}{\epsilon_\lambda^2}, \quad \frac{\delta \mathcal{Q}_3}{|\bar{\mathcal{Q}}|^3} \sim 0.22\, \epsilon_\lambda^{8/11}. \tag{38}$$

D. Charge cumulants

In addition to the charge moments one might be interested in the charge cumulants $\mathcal{K}_n = \langle\langle \hat{Q}^n \rangle\rangle$; the latter can be expressed through a combination of charge moments $\mathcal{Q}_m$ with $m \leqslant n$, for example,

$$\mathcal{K}_3 = \mathcal{Q}_3 - 3\mathcal{Q}_2\mathcal{Q}_1 + 2\mathcal{Q}_1^3. \tag{39}$$

Given a grid $\Lambda_{n,p} = \{\lambda_1, \ldots, \lambda_{k+p}\}$ of $k+p$ measuring points, one has to measure all charge moments $\mathcal{Q}_m$ with $m \leqslant n$. The most imprecise measurement in the above combination is given by the measurement of the highest charge moment $\mathcal{Q}_n$, hence this measurement has to be fully optimized with respect to the number of measurement proportions r_j as well as optimal coupling strengths λ_j. As follows from Eq. (29), the optimal value of λ_0 for each $\mathcal{Q}_m$ measurement with $m \leqslant n$ is given by

$$\bar{\lambda}_0^{(m)} \sim B_{m,p+n-m} |\bar{Q}|^{-1} \left[\frac{g(\epsilon) v_m}{\sqrt{N}} \right]^{1/(2n+2p-m+2)}. \tag{40}$$

The precision scaling in N involves only small exponents $1/(2n+2p-m+2)$ and thus all couplings $\bar{\lambda}_0^{(m)}$ are of the same order as $\bar{\lambda}_0^{(n)}$. The lower charge moments with $m < n$ then can be measured using the same grid $\Lambda_{n,p}$ and hence the same data $\tilde{\chi}(\lambda_j)$ with different weights $w_{\lambda_j}^{(n)}$. Finally, as the main contribution to the measurement error of $\mathcal{K}_n$ originates from the measurement error of the largest charge moment, we have

$$\delta \mathcal{K}_n \sim \delta \mathcal{Q}_n \tag{41}$$

with an optimized $\delta \mathcal{Q}_n$.

IV. CONCLUSION

In this paper, we have derived an optimized strategy for measuring the charge moments $\mathcal{Q}_n = \langle \hat{Q}^n \rangle$ (and hence the full counting statistics) in the random charge transfer across a mesoscopic device. These moments appear as derivatives of the generating function $\chi(\lambda)$, which can be measured with the help of a qubit performing Ramsey sequences at couplings λ. The derivatives of $\chi(\lambda)$ can be determined with the help of finite-difference formulas involving a set of measurements at different couplings λ_j, $j = 1, \ldots k+p$, with a minimal number of couplings $k = \lceil n/2 \rceil$ and $p \geqslant 0$ additional grid points. Given a total number N of Ramsey sequences, we have found the optimal distribution N_j of such measurements among the different couplings λ_j. For an equidistant grid, we have found the optimal grid separation $\bar{\lambda}_0$ and the exponent α of the precision scaling, $\delta \mathcal{Q}_n \propto N^{-\alpha}$. The typical coupling $\bar{\lambda}_0$ then generates a rotation $\varphi \sim 2\pi$ on the passage of the average charge $\bar{Q}$ during a Ramsey sequence, $\bar{Q}\bar{\lambda}_0 \sim \varphi/2\pi \sim 1$. The precision exponent $\alpha_{n,p}$ depends on the order n of the moment and the number p of additional grid points. Higher moments come with a poor scaling $\alpha_{n,0} = 1/(n+2)$ for the minimal grid with $p = 0$. On the other hand, choosing a large p is beneficial and allows one to approach the standard quantum limit $\alpha_{\mathrm{sql}} = 1/2$. The best set of couplings λ_j is not equidistant; unfortunately, finding this grid requires a numerical optimization. Such an optimization, as well as the determination of all other relevant quantities and numericals, has been done for the measurement of the third-order moment $\mathcal{Q}_3$. Another requirement is the precise knowledge of the couplings λ_j, as a relative imprecision ϵ_λ of the couplings λ_j limits the number N of useful measurements to a value $\bar{N} \propto 1/\epsilon_\lambda^2$. An interesting observation is that the nonequidistant optimized grid provides a better precision with fewer measurements as compared with the equidistant grid, although the difference is small [see Eqs. (37) and (38)].

Let us also discuss a few more subtle issues related to the measurement of the full counting statistics. First, we point out that the measured probability function or correlators depends on the type of qubit. E.g., a flux qubit measures the passage of directed charge (plus for right-moving, minus for left-moving) and hence quantifies the statistics of the net transferred charge. On the other hand, a charge qubit accumulates the signal from passing charge independent of its direction of motion and hence provides a characterization of the total charge transferred across the detector (in any direction); both quantities are measured perfectly well with the above recipe. It is then the experimenter who has to decide about the appropriate type of qubit that measures the quantity of interest.

A second issue is the location of the qubit detector, close or far away from the scattering region at $x = 0$. This question relates to some fundamental concerns that appeared very early on in the context of extending the transport characteristic beyond the noise correlator. In fact, different results have been obtained for the third-order cumulant, once the quantum

TABLE IV. Coefficients $E_{3,p}$ quantifying the accuracy $\delta \mathcal{Q}_3$ under uniform variation $\epsilon_\lambda = \delta\lambda_j/\lambda_j$ of the couplings λ_j.

Λ	$E_{3,0}$	$E_{3,1}$	$E_{3,2}$	$E_{3,3}$
Λ^{eq}	1.12	1.91	2.49	2.94
Λ^{opt}	0.55	0.76	0.86	0.91

binomial expression [11] $\langle\langle Q^3\rangle\rangle_q \propto -2T^2(1-T)$ when no time ordering was imposed or when placing the qubit near the scatterer [35], while the classical binomial result [12,14] $\langle\langle Q^3\rangle\rangle_c \propto T(1-T)(1-2T)$ has been found when time ordering was applied as prescribed through the inclusion of a spin detector into the description. The problem has been resolved recently [33] with the demonstration that the classical binomial result applies everywhere, far away as well as close to the scatterer, at least for the case of a spin or flux qubit device.

Another remark concerns the relation of measuring the FCS to the problem of quantum counting [31,32], where a qubit register of K qubits with coupling strengths $\lambda_j = \pi/2^{j-1}$, $j = 1,\ldots,K$ can be used to find the precise number of particles $m < 2^K$ that has been transmitted during a time t. Repeating the measurement many times and averaging then allows one to find the FCS $P_t(m)$ as well. However, in this case, the strongest coupling $\lambda_1 = \pi$ rotates the qubit $j = 1$ by π on passage of a single electron, so much stronger couplings are required than in the present protocol where $\lambda_0 \sim 1/\bar{Q}$. Furthermore, quantum counting and subsequent averaging provide much more information than needed if the goal is the measurement of a cumulant $\mathcal{Q}_n$.

ACKNOWLEDGMENTS

We acknowledge financial support from the Swiss National Science Foundation through the National Center of Competence in Research on Quantum Science and Technology, the Pauli Center for Theoretical Studies at ETH Zurich, and Russian Foundation for Basic Research Grant No. 14-02-01287.

[1] R. Landauer, IBM J. Res. Dev. **1**, 223 (1957).
[2] D. S. Fisher and P. A. Lee, Phys. Rev. B **23**, 6851 (1981).
[3] Y. Imry, in *Directions in Condensed Matter Physics*, edited by G. Grinstein and G. Mazenko (World Scientific, Singapore, 1986), p. 101.
[4] M. Büttiker, IBM J. Res. Dev. **32**, 63 (1988).
[5] G. B. Lesovik, Pis'ma Zh. Eksp. Teor. Fiz. **49**, 513 (1989) [JETP Lett. **49**, 592 (1989)].
[6] M. Büttiker, Phys. Rev. Lett. **65**, 2901 (1990).
[7] T. Martin and R. Landauer, Phys. Rev. B **45**, 1742 (1992).
[8] Ya.M. Blanter and M. Büttiker, Phys. Rep. **336**, 1 (2000).
[9] G. B. Lesovik and I. A. Sadovskyy, Usp. Fiz. Nauk **181**, 1041 (2011) [Phys. Usp. **54**, 1007 (2011)].
[10] Note that the measurement of FCS differs from the measurement of current correlators, e.g., current noise or higher-order correlators. The latter involves time-resolved or finite frequency measurements. The FCS relates to the system's low-frequency properties, e.g., zero-frequency noise, in the long-time limit.
[11] L. S. Levitov and G. B. Lesovik, Pis'ma Zh. Eksp. Teor. Fiz. **55**, 534 (1992) [JETP Lett. **55**, 555 (1992)].
[12] L. S. Levitov and G. B. Lesovik, Pis'ma Zh. Eksp. Teor. Fiz. **58**, 225 (1993) [JETP Lett. **58**, 230 (1993)].
[13] D. A. Ivanov and L. S. Levitov, Pis'ma Zh. Eksp. Teor. Fiz. **58**, 450 (1993) [JETP Lett. **58**, 461 (1993)].
[14] L. S. Levitov, H. W. Lee, and G. B. Lesovik, J. Math. Phys. **37**, 4845 (1996).
[15] B. A. Muzykantskii and D. E. Khmelnitskii, Phys. Rev. B **50**, 3982 (1994).
[16] W. Belzig and Y. V. Nazarov, Phys. Rev. Lett. **87**, 197006 (2001).
[17] A. V. Andreev and E. G. Mishchenko, Phys. Rev. B **64**, 233316 (2001).
[18] D. A. Bagrets and Yu. V. Nazarov, Phys. Rev. B **67**, 085316 (2003).
[19] F. Hassler, M. V. Suslov, G. M. Graf, M. V. Lebedev, G. B. Lesovik, and G. Blatter, Phys. Rev. B **78**, 165330 (2008).
[20] A. Komnik and G. W. Langhanke, Phys. Rev. B **90**, 165107 (2014).
[21] Y. Utsumi, O. Entin-Wohlman, A. Aharony, T. Kubo, and Y. Tokura, Phys. Rev. B **89**, 205314 (2014).
[22] P. Virtanen and F. Giazotto, AIP Advances **5**, 027140 (2015).
[23] B. Reulet, J. Senzier, and D. E. Prober, Phys. Rev. Lett. **91**, 196601 (2003).
[24] Y. Bomze, G. Gershon, D. Shovkun, L. S. Levitov, and M. Reznikov, Phys. Rev. Lett. **95**, 176601 (2005).
[25] A. V. Timofeev, M. Meschke, J. T. Peltonen, T. T. Heikkilä, and J. P. Pekola, Phys. Rev. Lett. **98**, 207001 (2007).
[26] W. Lu, Z. Q. Ji, L. Pfeiffer, K. W. West, and A. J. Rimberg, Nature (London) **423**, 422 (2003).
[27] R. Schleser, E. Ruh, T. Ihn, K. Ensslin, D. C. Driscoll, and A. C. Gossard, Appl. Phys. Lett. **85**, 2005 (2004).
[28] L. M. K. Vandersypen, J. M. Elzerman, R. N. Schouten, L. H. Willems van Beveren, R. Hanson, and L. P. Kouwenhoven, Appl. Phys. Lett. **85**, 4394 (2004).
[29] S. Gustavsson, R. Leturcq, B. Simovic, R. Schleser, T. Ihn, P. Studerus, K. Ensslin, D. C. Driscoll, and A. C. Gossard, Phys. Rev. Lett. **96**, 076605 (2006).
[30] G. B. Lesovik, F. Hassler, and G. Blatter, Phys. Rev. Lett. **96**, 106801 (2006).
[31] G. B. Lesovik, M. V. Suslov, and G. Blatter, Phys. Rev. A **82**, 012316 (2010).
[32] M. V. Suslov, G. B. Lesovik, and G. Blatter, Phys. Rev. A **83**, 052317 (2011).
[33] S. Bachmann, G. M. Graf, and G. B. Lesovik, J. Stat. Phys. **138**, 333 (2009); V. Beaud, G. M. Graf, A. V. Lebedev, and G. B. Lesovik, *ibid.* **153**, 177 (2013).
[34] B. Fornberg, Math. Comp. **51**, 699 (1988).
[35] K. V. Bayandin, A. V. Lebedev, and G. B. Lesovik, Zh. Eksp. Teor. Fiz. **133**, 140 (2008) [JETP **106**, 117 (2011)].